IDETC2020-22369

APPLICATIONS OF POLYNOMIAL CHAOS-BASED COKRIGING TO SIMULATION-BASED ANALYSIS AND DESIGN UNDER UNCERTAINTY

Jethro Nagawkar

Department of Aerospace Engineering Iowa State University Ames, Iowa, 50011 Email: jethro@iastate.edu

Leifur Leifsson*

Department of Aerospace Engineering lowa State University Ames, lowa, 50011 Email: leifur@iastate.edu

ABSTRACT

This paper demonstrates the use of the polynomial chaosbased Cokriging (PC-Cokriging) on various simulation-based problems, namely an analytical borehole function, an ultrasonic testing (UT) case and a robust design optimization of an airfoil case. This metamodel is compared to Kriging, polynomial chaos expansion (PCE), polynomial chaos-based Kriging (PC-Kriging) and Cokriging. The PC-Cokriging model is a multivariate variant of PC-Kriging and its construction is similar to Cokriging. For the borehole function, the PC-Cokriging requires only three high-fidelity samples to accurately capture the global accuracy of the function. For the UT case, it requires 20 points. Sensitivity analysis is performed for the UT case showing that the F-number has negligible effect on the output response. For the robust design case, a 75 and 31 drag count reduction is reported on the mean and standard deviation of the drag coefficient, respectively, when compared to the baseline shape.

INTRODUCTION

The use of physics-based simulation models is important in engineering, design and analysis. Examples of engineering areas where simulations play an important role include nondestructive testing (NDT) and aerodynamic design optimization.

NDT refers to the process of evaluating, inspecting and testing a part without physically damaging it [1]. NDT measurements depends on input variability parameter such as probe an-

gle and location. Some of these parameters have a higher effect on the output response. To determine how much of each input parameter has on the response, sensitivity analysis can be performed [2, 3]. In this work, global sensitivity analysis using Sobol' indices [4,5] is used. Traditional NDT methods have used finite element methods [6] and boundary element methods [7]. Unfortunately, for sensitivity analysis, in order to propagate variability parameters to output responses, a large number of model evaluations is needed, which can be impractical.

Aerodynamic shape optimization problems have typically focused on deterministic cases, where the use of gradient-based search method with adjoints are widely used [8–12]. Robust design optimization cases have also been performed, but have used metamodeling methods to handle the uncertainties [13, 14]. Performing robust design optimization is typically more expensive than its deterministic counterpart, owning to an increased number of model evaluations to allow for the propagation of input uncertainties to the model responses. This makes using physics-based simulation models challenging.

To reduce this computational cost, metamodeling methods can be used [15]. A computationally cheap metamodel replaces a costly physics-based model. Data-fit methods [16] and multifidelity methods [17] are two classes of metamodeling. A response surface is fitted though model evaluations at high-fidelity sample points in data-fit methods. In multifidelity methods, low-fidelity model evaluations can be used to enhance the prediction at a limited number of high-fidelity model evaluations.

In this work, the PC-Cokriging model developed by Du and

^{*}Address all correspondence to this author.

Leifsson [18] is used to perform sensitivity analysis on an UT benchmark case as well as a robust design optimization of an airfoil under uncertainly in Mach number. The PC-Cokriging model is also applied to an eight variable analytical borehole function [19]. PC-Cokriging is a multivariate version of the PC-Kriging model [18]. The global polynomial trend function in the Kriging metamodel is replaced with PCE to construct the PC-Kriging [20] metamodel. PCE captures the global trend well while the Kriging model the local deviations. PC-Cokriging is compared to other state-of-the-art metamodels, namely, Kriging [21], PCE [22], PC-Kriging [20] and Cokriging [23] to compare its performance as it combines the advantages of these metamodels.

This paper is organized in the following way. The next section describes the methods used to construct the PC-Cokriging metamodel and describes both the sensitivity analysis using Sobol' indices as well as optimization using this metamodel. In the following section, the PC-Cokriging model is applied to the three simulation-based problems. This paper then ends with conclusions and future work.

METHODS

In this section, the methods used to construct the PC-Cokriging metamodel is described. This section begins by outlining the multifidelity metamodeling algorithm, followed by the sampling plan, the construction of the metamodel, and its validation. The use of the metamodel for both sensitivity analysis as well as optimization is explained at the end of this section.

Multifidelity Metamodel Algorithm

The metamodel-based analysis flowchart is shown in Fig. 1. The input design/variability space first needs to be sampled, represented by X in Fig. 1, to generate the training data used to construct the metamodel. Two separate sets of data (\mathbf{x}_c and \mathbf{x}_e) are used to construct the low and high-fidelity metamodels by evaluating the responses (\mathbf{y}_c) and \mathbf{y}_e from the low and high-fidelity physics-based models, respectively. These metamodels are then combined to construct the multifidelity metamodel. In Fig. 1, y represents the combined observations of y_c and y_e , whereas $\hat{\mathbf{y}}_e$ is the metamodel prediction. To validate the global accuracy of the metamodel, a separate set of high-fidelity data, known as testing data, is used. The accuracy is measured using the root mean squared error (RMSE). This procedure needs to be redone multiple times to satisfy the testing criteria. Note that each time the amount of training data used is increased during resampling. On meeting the required global accuracy, this metamodel can be used for either sensitivity analysis or to find the optimum.

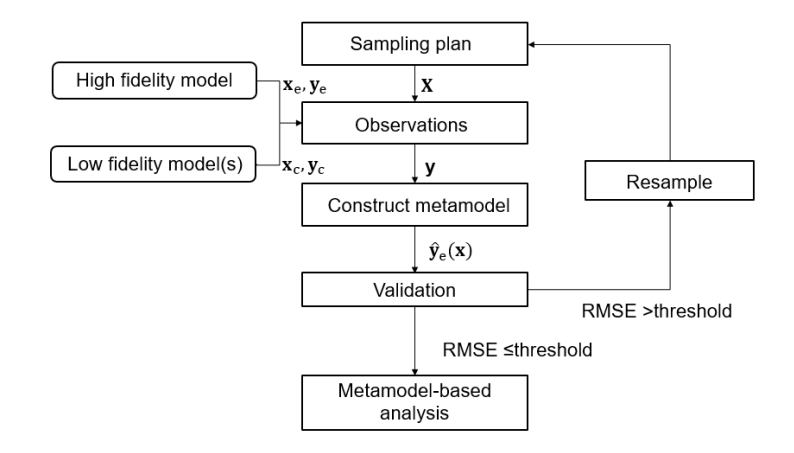


FIGURE 1. FLOWCHART OF THE PC-COKRIGING METAMODEL-BASED ANALYSIS.

Sampling Plan

The first step involved in constructing the metamodel is sampling. Sampling is the process of selecting discrete samples in the variable space [15]. In this study, the training data is generated using the Latin Hypercube sampling (LHS) [15] method. The number of high-fidelity samples generated is typically lower than those of the low-fidelity samples. This is due to the high computational cost required to evaluate the high-fidelity physics-based model. To generate the testing data, either the LHS method or the Monte Carlo sampling (MCS) [24] method is used.

Metamodeling

This study uses the PC-Cokriging model developed by Du and Leifsson [18]. The PC-Cokriging model is generated by combing metamodels, starting with the Kriging model [15], given by

$$M^{KR}(\mathbf{X}) = \mathbf{g}^{T}(\mathbf{X})\boldsymbol{\gamma} + \sigma^{2}Z(\mathbf{X}), \tag{1}$$

where $\mathbf{X} \in \mathbb{R}^m$ is the vector of m-dimensional input variability parameters. The first term is the global trend term and the second term is the local deviation term. $\mathbf{g}^T(\mathbf{X})$ is a set of regression basis terms and $\boldsymbol{\gamma}$ is a constant. $\boldsymbol{\sigma}^2$ is the constant variance of the Gaussian process $Z(\mathbf{X})$ with zero mean and unit variance. The Matern-5/2 [25] function is used as the correlation term in $Z(\mathbf{X})$, in this study.

The PC-Kriging model [20] uses PCE [22] as the global trend term and is given by

$$M^{PCK}(\mathbf{X}) = \boldsymbol{\alpha}^T \mathbf{\Phi}(\mathbf{X}) + \sigma^2 Z(\mathbf{X}). \tag{2}$$

Here, Φ is a set of orthogonal polynomial basis function and

 α is a constant. PC-Kriging combines the advantage of the PCE model, which captures the global behaviour of the computational model well and the Kriging model, which captures the local variations well.

Cokriging [23] is a fusion based model which combines information from multiple levels of fidelity to enhance prediction accuracy, especially in the presence of limited amount of high-fidelity data. In this work, information from two levels of fidelity is used. First, a Kriging model $(M_{LF}^{KR}(\mathbf{X}))$ is created using only low-fidelity data, followed by a second Kriging model $(M_{Diff}^{KR}(\mathbf{X}))$ on the difference of the high and low-fidelity data. The generic form of a Cokriging model is given by [23]

$$M^{CoK}(\mathbf{X}) = \rho M_{LF}^{KR}(\mathbf{X}) + M_{Diff}^{KR}(\mathbf{X}), \tag{3}$$

where ρ is a constant scaling factor.

The PC-Cokriging model [18] is a multivariate version of the PC-Kriging model and is constructed similar to the Cokriging model and is given by

$$M^{PC-CoK}(\mathbf{X}) = \rho M_{LF}^{PCK}(\mathbf{X}) + M_{Diff}^{PCK}(\mathbf{X}). \tag{4}$$

Here, $M_{\mathrm{LF}}^{PCK}(\mathbf{X})$ and $M_{\mathrm{Diff}}^{PCK}(\mathbf{X})$ are the PC-Kriging model on the low-fidelity and the difference between the low and high-fidelity data, respectively.

Validation

In this work, the global accuracy of the metamodel is measured using the RMSE, which is given by

RMSE =
$$\sqrt{\sum_{i=1}^{n_t} (\hat{y}_{testing}^{(i)} - y_{testing}^{(i)})^2 / n_t}$$
, (5)

and the normalized RMSE (NRMSE), given by

$$NRMSE = RMSE/(max(\mathbf{y}_{testing}) - min(\mathbf{y}_{testing})), \qquad (6)$$

where n_t is the total number of testing data. $\hat{y}_{testing}^{(i)}$ and $y_{testing}^{(i)}$ are the metamodel estimation and high-fidelity observation of the i^{th} testing point, respectively. The maximum and minimum high-fidelity values from the testing data are $\max(\mathbf{y}_{testing})$ and $\min(\mathbf{y}_{testing})$, respectively. In this work, $1\%\sigma_{testing}$ (standard deviation of testing points) is considered as an acceptable global accuracy.

Metamodel-Based Sensitivity Analysis

For the NDE case, the constructed metamodel is used to perform sensitivity analysis, using Sobol' indices [4]. Sensitivity

analysis is used to determine how much each variability parameter affects the model response.

Consider a black box model given by,

$$M(\mathbf{X}) = f(\mathbf{X}),\tag{7}$$

where X is a m random variable input vector. Decomposing this equation gives [5]

$$M(\mathbf{X}) = f_0 + \sum_{i=1}^{m} f_i(X_i) + \sum_{i< j}^{m} f_{i,j}(X_i, X_j) + \dots + f_{1,2,\dots,m}(X_1, X_2, \dots, X_m),$$
(8)

where f_0 is a constant, and f_i is a function of X_i . These terms are orthogonal and can then be decomposed in terms of conditional expected values given by [5]

$$f_0 = \mathbb{E}(M(\mathbf{X})),\tag{9}$$

$$f_i(X_i) = \mathbb{E}(M(\mathbf{X})|X_i) - f_0, \tag{10}$$

$$f_{i,j}(X_i, X_j) = \mathbb{E}(M|X_i, X_j) - f_0 - f_i(X_i) - f_j(X_j), \tag{11}$$

and so on. The variance of (8) is then [5]

$$\mathbb{V}ar(M(\mathbf{X})) = \sum_{i=1}^{m} V_i + \sum_{i< j}^{m} V_{i,j} + \dots + V_{1,2,\dots,m},$$
(12)

where

$$V_i = \mathbb{V}ar_{X_i}(\mathbb{E}_{\mathbf{X}_{\alpha,i}}(M(\mathbf{X})|X_i)), \tag{13}$$

$$V_{i,j} = \mathbb{V}ar_{X_{i,j}}(\mathbb{E}_{\mathbf{X}_{\sim i,j}}(M(\mathbf{X})|X_i,X_j)) - V_i - V_j, \tag{14}$$

and so on, where the set of all variables except X_i is denoted by $\mathbf{X}_{\sim i}$.

The first-order Sobol' indices are given by [4]

$$S_i = \frac{V_i}{\mathbb{V}ar(M(\mathbf{X}))},\tag{15}$$

and the total-effect Sobol' indices are given by [4]

$$S_{T_i} = 1 - \frac{\mathbb{V}ar_{\mathbf{X}_{\sim i}}(\mathbb{E}_{X_i}(M(\mathbf{X})|\mathbf{X}_{\sim i}))}{\mathbb{V}ar(M(\mathbf{X}))}.$$
 (16)

TABLE 1. VARIABILITY PARAMETERS AND THEIR DISTRIBUTION FOR THE BOREHOLE FUNCTION [19].

Variability Parameters	Distribution
radius of borehole, $r_w(m)$	N(0.1, 0.0161812 ²)
radius of influence, $r(m)$	$LogN(7.71, 1.0056^2)$
transmissivity of upper aquifer, $T_u(m^2/yr)$	U(63070, 115600)
potentiometric head of upper aquifer, $H_u(m)$	U(990, 1110)
transmissivity of lower aquifer, $T_l(m^2/yr)$	U(63.1, 116)
potentiometric head of lower aquifer, $H_l(m)$	U(700, 820)
length of borehole, $L(m)$	U(1120, 1680)
hydraulic conductivity of borehole, $K_w(m/yr)$	U(9855, 12045)

Metamodel-Based Optimization

To find the optimum from the generated metamodel, the sequential least squares programming (SLSQP) gradient-based optimizer available in SciPy [26] is used. 40 started points are selected from which the SLSQP algorithm begins its search. These starting points are generated using LHS. This is done to find the best local minimum.

NUMERICAL EXAMPLES

In this study, the PC-Cokriging model is applied to three different simulation-driven engineering design problems. The first is an eight variable analytical function, the borehole function. The second, an ultrasonic testing benchmark case and the third is robust optimization of an airfoil under uncertainty in Mach number. The PC-Cokriging model is compared to other state-of-the-art metamodels, namely, Kriging, PCE, PC-Kriging and Cokriging.

Borehole Function

The borehole function [19] is an eight variable problem used to model flow of water through a borehole and is given by

$$f_{\rm HF}(\mathbf{x}) = \frac{2\pi T_u (H_u - H_l)}{ln(r/r_w) \left(1 + \frac{2LT_u}{ln(r/r_w)r_w^2 K_w} + \frac{T_u}{T_l}\right)}.$$
 (17)

Each of the variability parameter and its distribution is given in Tab. 1. The low fidelity model developed by Xiong et al. [27] is used and is given by

TABLE 2. BOREHOLE FUNCTION METAMODELING COST.

Metamodel	HF sample cost
Kriging	300
PCE	100
PC-Kriging	100
Cokriging	200*
PC-Cokriging	3*

^{*}Plus 170 LF training points

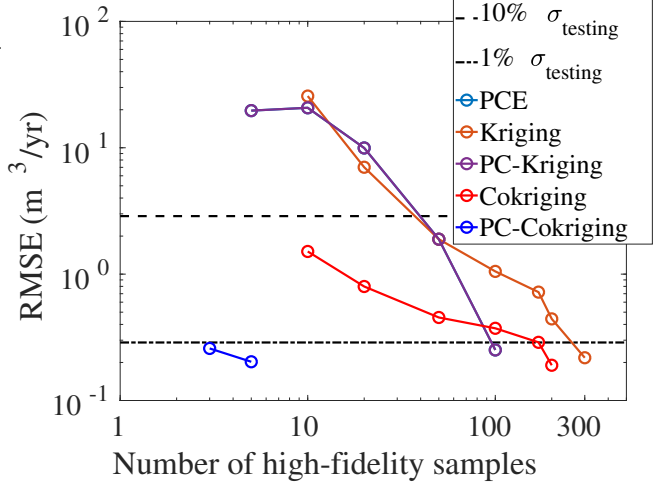


FIGURE 2. BOREHOLE FUNCTION METAMODEL VALIDATION.

$$f_{\rm LF}(\mathbf{x}) = \frac{5T_u(H_u - H_l)}{ln(r/r_w)\left(1.5 + \frac{2LT_u}{ln(r/r_w)r_w^2K_w} + \frac{T_u}{T_l}\right)}.$$
 (18)

Results Table 2 shows the number of high fidelity samples required by each metamodel to reach the global accuracy of $1\%\sigma_{testing}$. This accuracy is measure using 1,000 MCS generated testing points. Note that the multifidelity models use an additional of 170 low-fidelity sample points. PC-Cokriging far outperforms the other models requiring only 3 high-fidelity data points. PCE and PC-Kriging follow the exact same trend (Fig. 2) and require 100 high-fidelity points to meet the 1% threshold, while Cokriging and Kriging require 200 and 300, respectively. This case assumes that sampling the low-fidelity model is computationally efficient and its cost is negligible.

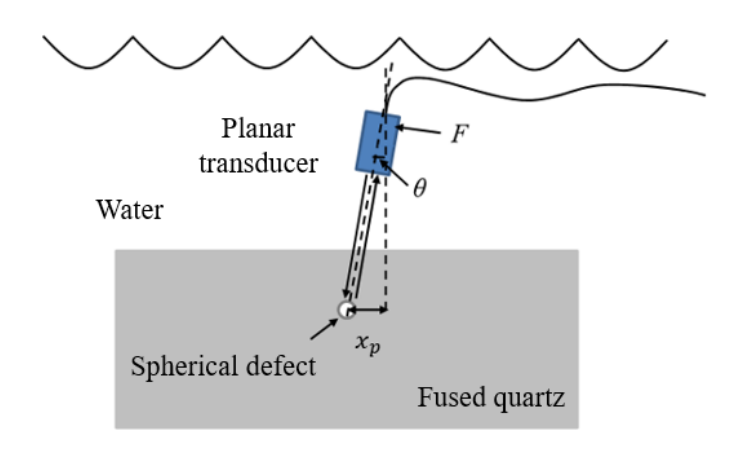


FIGURE 3. SETUP FOR THE ULTRASONIC TESTING CASE.

TABLE 3. VARIABILITY PARAMETERS AND THEIR DISTRIBUTION FOR THE ULTRASONIC TESTING CASE.

Variability Parameters	Case 1
θ (deg)	$N(0, 0.5^2)$
x (mm)	U(0, 1)
F	U(13, 15)

Ultrasonic Testing Case

In this study the spherically-void-defect under planar transducer ultrasonic testing benchmark case developed by the World Federal Nondestructive Evaluation Center [28] is used. The five metamodel are compared in terms of cost required to reach the global accuracy of $1\%\sigma_{\text{testing}}$. Sensitivity analysis using these metamodels are also performed.

Problem Setup The setup for the UT benchmark case is shown in Fig. 3. The three variability parameters, namely, the probe angle (θ) , the x location of the probe (x_p) and the F-number (F) along with their corresponding distributions are shown in Tab. 3. For this study, the analytical model [29] is used as the high-fidelity model, while the Kirchhoff approximation is used as the low-fidelity one. The center frequency of the transducers are set to 5 MHz, while the density, the longitudinal and the shear wave speeds of the fused quartz block with spherical pore are $2,000 \ kg/m^3$, $5,969.4 \ m/s$ and $3,774.1 \ m/s$, respectively.

TABLE 4. ULTRASONIC TESTING CASE METAMODELING COST.

Metamodel	HF sample cost
Kriging	1000
PCE	120
PC-Kriging	56
Cokriging	48*
PC-Cokriging	20*

^{*}Plus 1000 LF training points

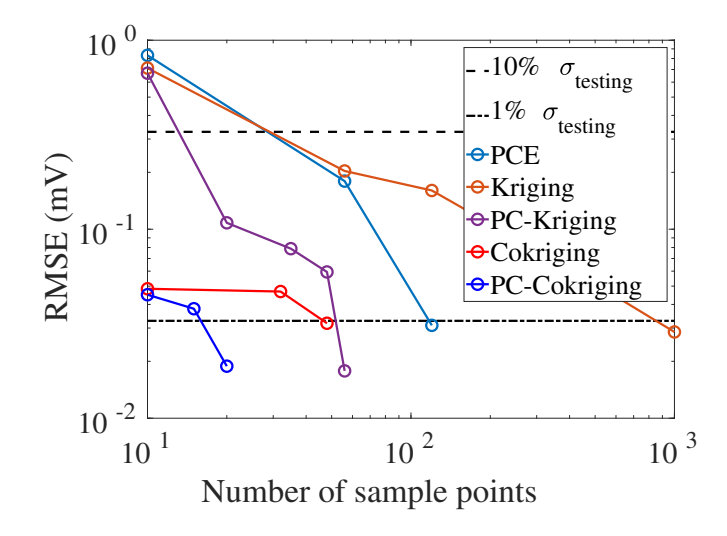


FIGURE 4. ULTRASONIC TESTING CASE METAMODEL VALIDATION (RMSE).

Results Figure 4 shows the variation of the RMSE for all the metamodels with increasing number of high-fidelity training points, for the defect of size 0.5 mm. PC-Cokriging outperform all the other metamodels and requires 20 high-fidelity samples to reach the 1% threshold. The computational cost of all the models are shown in Tab. 4. 1,000 additional low-fidelity samples are used to construct the multifidelity models. For this case we assume the cost of observing the low-fidelity sample is negligible.

To verify the accuracy of the metamodels for different defect sizes, the NRMSE is calculated. Figure 5 shows the variation of the NRMSE with increasing defect sizes. The NRMSE is nearly constant with respect to defect size and within $1\%\sigma_{testing}$. Similar to the previous case, 1,000 MCS generated testing points per

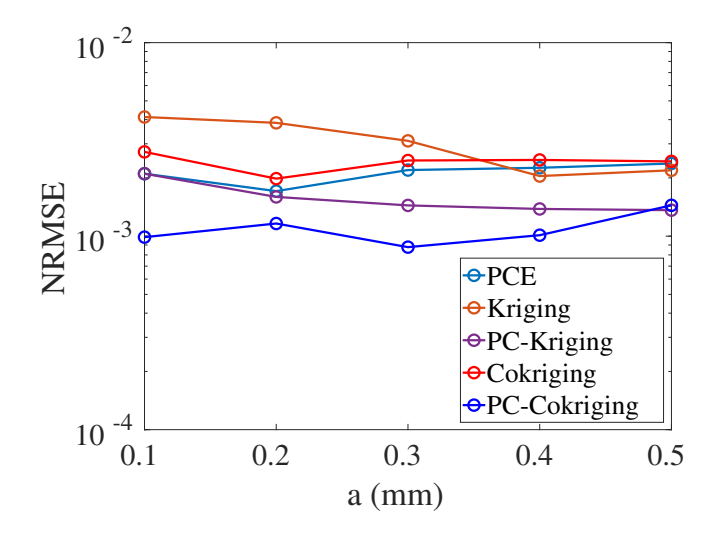


FIGURE 5. ULTRASONIC TESTING CASE METAMODEL VALIDATION (NRMSE).

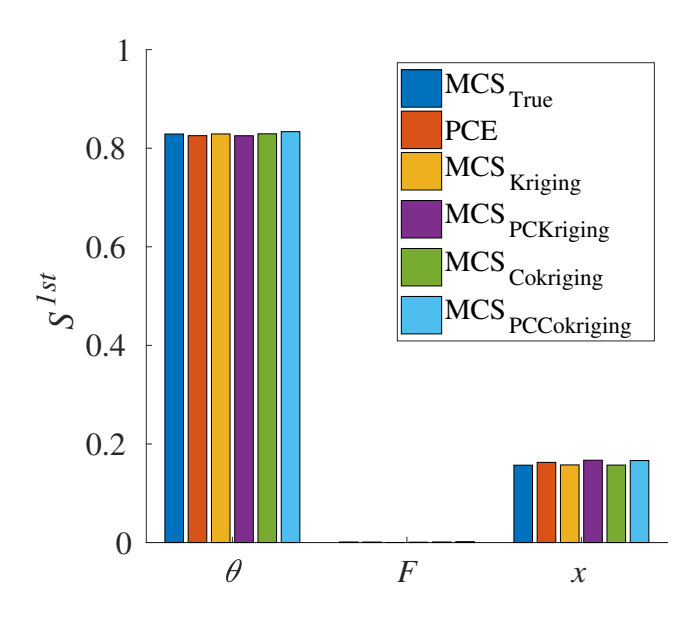


FIGURE 6. 1^{ST} ORDER SOBOL' INDICES FOR THE ULTRASONIC TESTING CASE.

defect size were used to measure the accuracy of the metamodel.

Figures 6 and 7 shows the 1st and total order Sobol' indices for the different metamodels. The results from the metamodels are compared the those obtaining from directly sampling the physics-based model. In all the models except PCE, 75,000 MCS were used to perform sensitivity analysis. In PCE, the coefficients are used to calculate these indices. The values of these

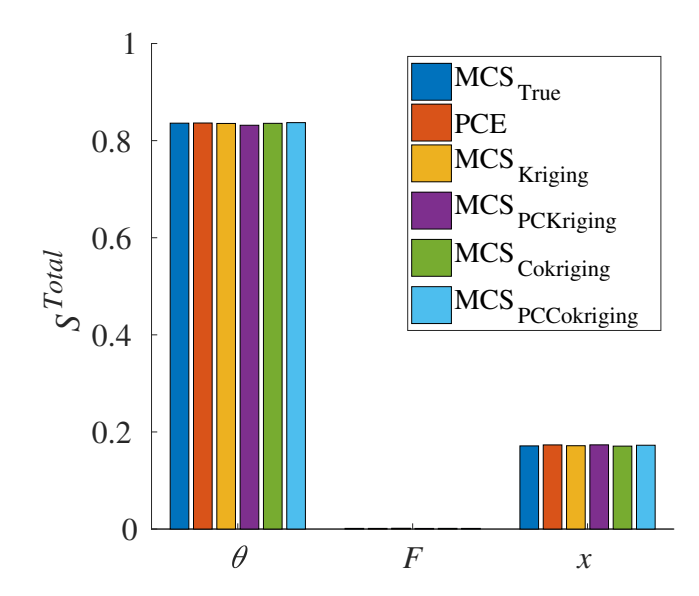


FIGURE 7. TOTAL ORDER SOBOL' INDICES FOR THE ULTRA-SONIC TESTING CASE.

indices match well for all the metamodels. Metamodel-based sensitivity analysis is highly efficient for this case as instead of evaluating the model response 75,000 times to get the Sobol's indices, the metamodels output these responses at little to no cost. The F-number has negligible effect on the model response. This method can be used as a precursor to experimental measurements, where the number experiments can be reduced by keeping the value of the F-number constant.

Robust Design Optimization

The final case is a robust design optimization of a RAE 2822 airfoil under uncertainty in the Mach number. This case is a modified version of benchmark case II developed by the AIAA Aerodynamic Optimization Design Discussion Group (ADODG). The five metamodels are constructed and used to find the minimum. The results from this robust optimization case are compared to the deterministic ADODG case II performed by Nagawkar et al. [30]. Note that the type of parameterization (B-spline) as well as the computational fluid dynamics (CFD) setup and validation is the same those by Nagawkar et al. [30]. The CFD simulations are performed using Stanford University Unstructured [31] and the mesh is generated using pyHyp¹ [9]. For this study, however, the bounds of the design variables are increased from $(1\pm15\%)\mathbf{x}_0$ to $(1\pm25\%)\mathbf{x}_0$. \mathbf{x}_0 is the baseline design variable values.

¹Developed at the MDOlab, University of Michigan

Problem Formulation In this case, the objective is to minimize the drag coefficient (C_d) of a RAE 2822 airfoil in viscous flow with the freestream Mach number (M_∞) varying uniformly in the range 0.725 to 0.743, subject to a fixed lift coefficient (C_l) of 0.824 as well as pitching moment coefficient (C_m) and cross-sectional area constraints (A).

The optimization problem is formulated as

$$\min_{1 \le \mathbf{x} \le \mathbf{u}} (\mu(C_d) + \boldsymbol{\omega} \cdot \boldsymbol{\sigma}(C_d)) \tag{19}$$

subject to the equality constraint

$$C_l = 0.824$$
 (20)

and inequality constraints

$$\mu(C_m) \ge -0.092\tag{21}$$

and

$$A \ge A_{baseline}$$
. (22)

x is the design variable vector, while **l** and **u** are the lower and upper bounds, respectively, of each design variable. μ and σ refer to the mean and standard deviation. ω is the weighting factor and is set to one for this case. A is the cross-sectional area of the airfoil non-dimensionalised with the square of the chord length (c). $A_{baseline}$ is the baseline area of the airfoil with a value of $0.07787c^2$.

Results For this case, two different metamodels were constructed for the objective function and the pitching moment constraint function. The variation of the RMSE with number of training points used to construct the metamodels is shown in Figs. 8 and 9, respectively. The multifidelity metamodel used an additional 1,604 low fidelity training points for this case. 115 high-fidelity testing points were used to measure the RMSE. The multifidelity metamodel show significant higher accuracy for the drag coefficient metamodels in presence of low amount of high-fidelity data as shown in Fig. 8. This is not the case for the pitching moment coefficient metamodel (Fig. 9). For both the cases, increasing the number of high-fidelity training points, decreases the difference in accuracy between the multifidelity and data-fit metamodels.

Figure 10 shows the variation of the drag coefficient with Mach number. The robust design case is compared to the deterministic case as well as the baseline shape. Significant reduction in both the mean and standard deviation of drag with

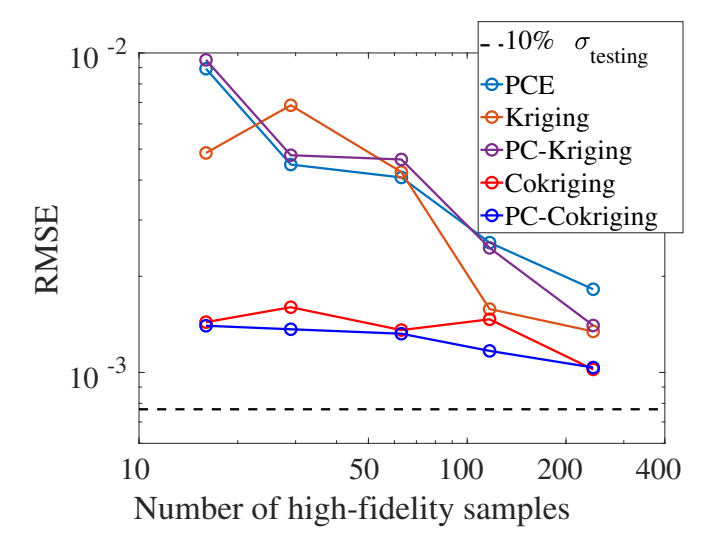


FIGURE 8. DRAG COEFFICIENT METAMODEL VALIDATION FOR THE OPTIMIZATION CASE.

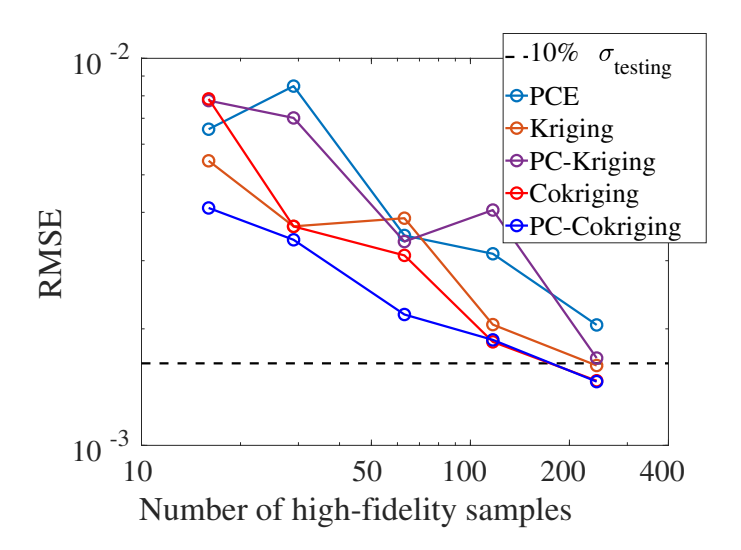


FIGURE 9. PITCHING MOMENT METAMODEL VALIDATION FOR THE OPTIMIZATION CASE.

respect to Mach number is noticed (Tab. 5). However, for the robust case, the standard deviation of the drag is around ten drag counts lower when compared to the deterministic optimization case. This shows that robust design optimization results in an airfoil that is less sensitive to the Mach number. The differences in airfoil shapes between the optimized and baseline shapes is shown in Fig. 11. Both the optimized shapes have a lower curvature on the suction side of the airfoil from the leading edge to around mid-chord. This shape reduces the acceleration of the flow over the suction side, resulting in a lower local Mach num-

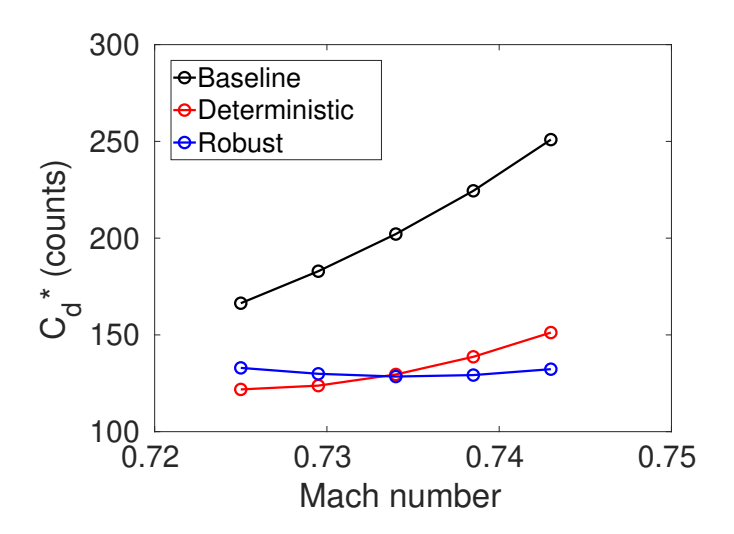


FIGURE 10. VARIATION OF DRAG COEFFICIENT WITH RESPECT TO MACH NUMBER: BASELINE V/S OPTIMIZED.

TABLE 5. ROBUST DESIGN OPTIMIZATION RESULTS.

Case	$\mu(C_d)$	$\sigma(C_d)$	$\Delta\mu(C_d)$	$\Delta\sigma(C_d)$	$\mu(C_m)$
Baseline	205.3	33.4	-	-	-0.099
Deterministic	133.0	12.1	72	21	-0.092
Robust	130.6	1.9	75	31	-0.090

 C_d is in drag counts.

One count is 1E-4

ber, which in turn reduces the shock strength, thereby reducing the drag. Small differences in the shape has significant effect on the drag as well as pressure coefficient on the airfoil as seen in Fig. 12. The optimized shapes for both the cases have not eliminated the shock completely, but has reduced its strength significantly.

CONCLUSION

The PC-Cokriging metamodel is applied to three different simulation-based engineering problems. This metamodel is compared to other state-of-the-art metamodels, namely, Kriging PCE, PC-Kriging and Cokriging. The PC-Cokriging metamodel is a multivariate version of PC-Kriging and its construction is similar to Cokriging. The PC-Kriging model uses PCE as the global trend function in Kriging. PC-Kriging combines the advantages of Kriging and PCE.

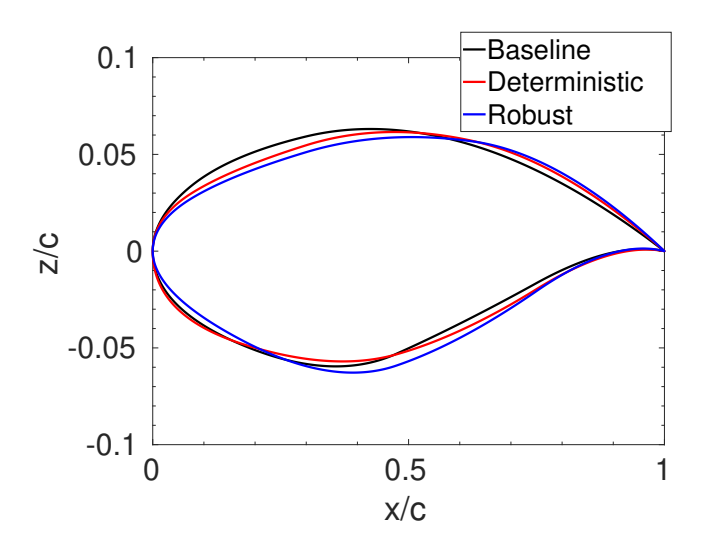


FIGURE 11. SHAPE COMPARISON: BASELINE V/S OPTI-MIZED.

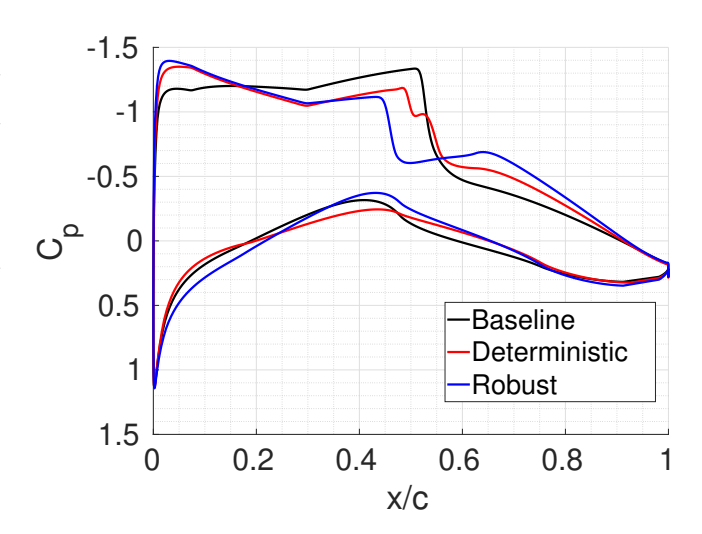


FIGURE 12. PRESSURE COEFFICIENT AT 0.734 MACH NUMBER: BASELINE V/S OPTIMIZED.

For the Borehole function, the PC-Cokriging metamodel required only three high-fidelity points to reach the target accuracy of $1\%\sigma_{testing}$. Its nearest competitors, PCE and PC-Kriging require 100 each. In the ultrasonic testing benchmark case, PC-Cokriging required 20 high-fidelity samples, while Cokriging required 48. For the final case, the trend of the PC-Cokriging model is similar to Cokriging. To reach the target accuracy of $1\%\sigma_{testing}$ more high-fidelity samples will be required to construct the metamodels. This will be done in future studies of this case.

Sensitivity analysis was performed for the ultrasonic testing case. All the metamodels show similar values for both the 1^{st} and total order Sobol' indices. The F-number has virtually no effect on the model response for this case. This information can be used as a precursor for setting up experiments for ultrasonic testing. For this case, the F-number can be neglected while performing experiments. More variability parameters will be included in future cases.

Robust design optimization was performed on a RAE 2822 airfoil under uncertainty in freestream Mach number. When compared to a deterministic optimization case, the robust case not only reduced the mean drag coefficient, but also made the drag coefficient virtually invariant with changing Mach number. The pressure coefficient was significantly affected for a relatively small change in airfoil shape, showing the importance of performing robust shape optimization. Future studies will include uncertainties in lift, pitching moment as well as thickness of the airfoil.

ACKNOWLEDGMENT

The authors of this paper are supported by NSF award number 1846862.

REFERENCES

- [1] Crawley, P., 2001. "Non-destructive testing current capabilities and future directions". *Journal of Material: Design and Applications*, **215**(4), pp. 213–223.
- [2] Lilburne, L., and Tarantola, S., 2009. "Sensitivity analysis of spatial models". *International Journal of Geographical Information Science*, 23, pp. 151–168.
- [3] Castillos, E., Conejo, A., Minguez, R., and Castillos, C., 2007. "A closed formula for local sensitivity analysis in mathematical programming". *Engineering Optimization*, 38, pp. 93–112.
- [4] Sobol', I., and Kucherekoand, S., 1993. "Sensitivity estimates for nonlinear mathematical models". *Mathematical Modelling and Computational Experiments*, 1, pp. 407–414.
- [5] Sobol', I., 2001. "Global sensitivity indices for nonlinear mathematical models and their monte carlo estimates". *Mathematics and Computers in Simulation*, 55, pp. 271–280
- [6] Zeng, Z., Udpa, L., and Udpa, S. S., 2009. "Finite-element model for simulation of ferrite-core eddy-current probe". *IEEE Transaction on Magnetics*, **46**, pp. 905–909.
- [7] Zhang, C., and Gross, D., 2002. "A 2D hyper singular time-domain traction BEM for transient elastodynamic crack analysis". *Wave Motion*, *35*, pp. 17–40.
- [8] Leung, T. M., and Zingg, D. W., 2012. "Aerodynamic shape

- optimization of wings using a parallel newton-krylov approach". *AIAA Journal*, *50*(3), pp. 540–550.
- [9] He, X., Li, J., Mader, C. A., Yildirim, A., and Martins, J. R. R. A., 2019. "Robust aerodynamic shape optimization from a circle to an airfoil". *Aerospace Science and Technology*, 87, pp. 48–61.
- [10] Secco, N. R., and Martins, J. R. R. A., 2019. "RANS-based aerodynamic shape optimization of a strut-braced wing with oversetmeshes". *Journal of Aircraft*, 56, pp. 217–227.
- [11] Yu, Y., Lyu, Z., Xu, Z., and Martins, J. R. R. A., 2018. "On the influence of optimization algorithm and initial design on wing aerodynamic shape optimization". *Aerospace Science and Technology*, 75, pp. 183–199.
- [12] Lyu, Z., Kenway, G. K., and Martins, J. R. R. A., 2015. "Aerodynamic shape optimization investigations of the common research model wing benchmark". *AIAA Journal*, *53*, pp. 968–985.
- [13] Shah, H., Hosder, S., Koziel, S., Tesfahunegn, Y. A., and Leifsson, L., 2015. "Multi-fidelity robust aerodynamic design optimization under mixed uncertainty". *Aerospace Science and Technology*, 45, pp. 17–29.
- [14] Bouhlel, M. A., Regis, N. B. R. G., and A. Otsmane, a. J. M., 2018. "Efficient global optimization for high-dimensional constrained problems by using the kriging models combined with the partial least squares method". *Engineering Optimization*, **0**, pp. 1–16.
- [15] Forrester, A. I. J., Sobester, A., and Keane, A. J., 2008. Engineering design via surrogate modelling: A practical guide. John Wiley and Sons, Ltd, United Kingdom.
- [16] Queipo, N. V., Haftka, R. T., Shyy, W., Goel, T., Vaidyanathan, R., and Tucker, P. K., 2005. "Surrogate-based analysis and optimization.". *Progress in Aerospace Sciences*, 21(1), pp. 1–28.
- [17] Peherstorfer, B., Wilcox, K., and Gunzburger, M., 2018. "Survey of multifidelity methods in uncertainty propagation, inference, and optimization". *Society for Industrial and Applied Mathematics*, **60**(3), pp. 550–591.
- [18] Du, X., and Leifsson, L., 2020. "Multifidelity modeling by polynomial chaos-based cokriging to enable efficient model-based reliability analysis of ndt systems". *Journal of Nondestructive Evaluation*, 1.
- [19] Harper, W. V., and Gupta, K. S., 1983. Sensitivity/uncertainty analysis of a borehole scenario comparing Latin Hypercube Sampling and deterministic sensitivity approaches. Technical report, Office of Nuclear Waste Isolation, Columbus, OH.
- [20] Schobi, R., Sudret, B., and Wairt, J., 2015. "Polynomial-chaos-based kriging". *International Journal of Uncertainty Quantification*, 5, pp. 193–206.
- [21] Krige, D. G., 1951. "Statistical approach to some basic mine valuation problems on the witwatersrand". *Journal of the Chemical, Metallurgical and Mining Engineering Soci-*

- ety of South Africa, 52(6), pp. 119-139.
- [22] Blatman, G., 2009. "Adaptive sparse polynomial chaos expansion for uncertainty propagation and sensitivity analysis". PhD Thesis, Blaise Pascal University, France.
- [23] Kennedy, M. C., and O'Hagan, A., 2000. "Predicting the output from a complex computer code when fast approximations are available". *Biometrika Trust*, 87(1), pp. 1–13.
- [24] Shapiro, A., 2003. "Monte carlo sampling methods". Handbooks in Operations Research and Management Science, 10, pp. 353–425.
- [25] Gneiting, T., Kleiber, W., and Schlather, M., 2010. "Matérn cross-covariance functions for multivariate random fields". *Journal of the American Statistical Association*, 105, pp. 1167–1177.
- [26] Virtanen, P., Gommers, R., Oliphant, T. E., Haberland, M., Reddy, T., Cournapeau, D., and Burovski, E., 2019. SciPy 1.0-Fundamental Algorithms for Scientific Computing in Python. See also URL http://arxiv.org/abs/1907.10121, August.
- [27] Xiong, S., Qian, P. Z., and Wu, J. C., 2013. "Sequental design and analysis of high-accuracy and low-accuracy computer codes". *Technometrics*, *55*(1), pp. 37–46.
- [28] Gurrala, P., Chen, K., Song, J., and Roberts, R., 2017. "Full wave modeling of ultrasonic NDE benchmark problems using Nystrom method". *Review of Progress in Quantitative Nondestructive Evaluation*, 36(1), pp. 1–8.
- [29] Schmerr, L., and Lester, W., 2016. Fundamentals of Ultrasonic Nondestructive Evaluation: A modeling approach. Springer International Publishing, Switzerland.
- [30] Nagawkar, J., Leifsson, L., and Du, X., 2020. "Applications of polynomial chaos-based cokriging to aerodynamic design optimization benchmark problems". AIAA Scitech 2020 Forum, 6-10 January, Orlando Florida.
- [31] Economon, T. D., Palacios, F., Copeland, S. R., Lukaczyk, T. W., and Alonso, J. J., 2015. "SU2: An open-source suite for multiphysics simulation and design". *AIAA Journal*, *54*(3), pp. 828–846.